

Nuclear Localization of ^{111}In After Intravenous Injection of [^{111}In -DTPA-D-Phe¹]-Octreotide in Patients with Neuroendocrine Tumors

Eva Tiensuu Janson, Jan-Erik Westlin, Ulf Öhrvall, Kjell Öberg, and Agneta Lukinius

Departments of Medical Sciences; Oncology, Radiology, and Clinical Immunology; Surgery; and Genetics and Pathology, University Hospital, Uppsala, Sweden

Treatment with tumor-targeting substances is currently being evaluated in clinical trials. For patients with neuroendocrine tumors expressing somatostatin receptors, the ^{111}In -labeled somatostatin analog [diethylenetriaminepentaacetic acid (DTPA)-D-Phe¹]-octreotide has been used with promising results. To further investigate the clinical effect of the injected conjugate, we analyzed the cellular distribution of ^{111}In by ultrastructural autoradiography. **Methods:** Seven patients with somatostatin receptor-expressing midgut carcinoid tumors scheduled for abdominal surgery were investigated by somatostatin receptor scintigraphy. During operation, tumor tissue samples and samples of normal intestine were collected, fixed, and processed for electron microscopy. A thin layer of film emulsion was applied on sections and after the exposure film was developed. The cellular distribution of silver precipitations indicating the presence of isotope was evaluated. **Results:** Cell surface receptor binding and internalization of [^{111}In -DTPA-D-Phe¹]-octreotide in the tumor cells was easily revealed by silver precipitations in the film. Multiple silver grains were seen at the plasma membrane, in the cytoplasmic area among secretory granules and vesicular compartments, and in the perinuclear area. Silver grains were also regularly located in the nucleus. For all patients, the silver precipitation patterns from ^{111}In decay were identical in all examined cells from removed tumors, and in most cells ^{111}In could be seen in the nucleus. The specificity of the silver reaction products is supported by the observation that enterocytes in intestinal tissue specimens from near the tumor did not show any silver grains and no background labeling was seen in the plastic. **Conclusion:** After internalization through the somatostatin receptor system, ^{111}In is translocated to the perinuclear area and into the nucleus. Whether the nuclide is still conjugated to the intact somatostatin analog or to part of it cannot be evaluated in this study. Despite the short irradiation range of ^{111}In , the nuclear localization can explain its clinical effectiveness. The results from this study suggest that [^{111}In -DTPA-D-Phe¹]-octreotide may act as a powerful tumor cell-targeting substance.

Key Words: autoradiography; carcinoid tumor; internalization; octreotide; somatostatin analog; somatostatin receptor; treatment

J Nucl Med 2000; 41:1514–1518

Somatostatin receptors belong to the 7-transmembrane receptor family with 5 different subtypes cloned (1–3). Somatostatin receptors are expressed in many different malignancies, including breast cancer and pituitary and neuroendocrine tumors (4,5). Because of the receptor expression, somatostatin analogs are used for medical treatment to reduce hormone levels and clinical symptoms and to scintigraphically visualize neuroendocrine tumors (6–8). Biodistribution studies of the somatostatin analog [^{111}In -diethylenetriaminepentaacetic acid (DTPA)-D-Phe¹]-octreotide (^{111}In -octreotide) show high uptake in neuroendocrine tumor cells, with a tumor-to-blood ratio of up to 200 in patients after intravenous injection of 100–200 MBq of the conjugate (9). Therapy with radioactive labeled somatostatin analogs as tumor-targeting molecules is currently being evaluated in several clinical studies, and objective responses after high-dose fractionated treatment with ^{111}In -octreotide have been reported for patients with neuroendocrine tumors (10–12).

^{111}In is a γ and Auger electron emitter in which the γ irradiation has too low an energy to explain tumor cell damage. Thus, the promising clinical effect has been attributed to the Auger electrons, which have an irradiation range of 50–1000 nm and an energy range of 0.5–25 keV (11). The short range has been considered to be a disadvantage because the ^{111}In molecule has to be very close to the tumor cell nucleus to exert its cytotoxic effect in the form of DNA double-strand damage (13). Examinations of the intracellular distribution of ^{111}In -octreotide in tumor cells from patients after an intravenous injection of the conjugate have thus been of interest, and a method for ultrastructural autoradiography of tumor specimens from these patients has been developed (14). With this method, the cellular localization of ^{111}In decay can be identified, and in this paper we report our initial results for 7 patients.

MATERIALS AND METHODS

Patients

Seven patients who had malignant midgut carcinoid tumors and were scheduled for abdominal surgery were included in this study (2 women, 5 men; age range, 42–70 y; median age, 54 y). Two days

Received May 12, 1999; revision accepted Sep. 21, 1999.

For correspondence or reprints contact: Eva Tiensuu Janson, MD, PhD, Department of Medical Sciences, University Hospital, S-751 85 Uppsala, Sweden.

before surgery, the patients received an intravenous injection of 200 MBq ^{111}In -octreotide, and 1 d before surgery, somatostatin receptor scintigraphy was performed to localize the tumor.

Surgery

During abdominal surgery, samples of primary and metastatic tumor tissue were collected. The histopathologic examination showed classic midgut carcinoid tumors in all patients, with positive immunohistochemical staining for chromogranin A and serotonin. For control purposes, adjacent normal intestinal tissue was also collected.

Samples of all tissue specimens were blotted dry and weighed. The samples, together with peripheral blood (1.2 mL), were analyzed in a scintillation well counter (1282 CompuGamma; LKB Wallac, Turku, Finland) calibrated for ^{111}In . Attempts were made to standardize specimen geometry. The tumor-to-blood and normal tissue-to-blood radioactivity ratios were calculated with standardization for weight.

Somatostatin Receptor Scintigraphy

Somatostatin receptor scintigraphy was performed as described in an earlier report (15). Briefly, the patient received an intravenous injection of 200 MBq ^{111}In -octreotide (Mallinckrodt, Inc.; Petten, The Netherlands). Anteroposterior whole-body images were collected the day after injection, and SPECT was performed over the abdomen using a scintillation SPECT gamma camera equipped with a medium-energy general-purpose collimator (Nuclear Diagnostics, Hägersten, Sweden). Original data for the SPECT images were collected using a 64-step rotation of 360° in a 64×64 word matrix. Energy windows of 173 and 247 keV ($\pm 10\%$) were used. The collection time for each angle was 40 s, giving a total of approximately 30,000 counts per angle. A Wiener filter was applied to the original data for the reconstruction of SPECT images. The patients were immobilized using vacuum pillows to avoid motion artifacts. However, no correction for respiratory movement was performed.

Ultrastructural Autoradiography

Immediately after tumor dissection, small, randomly collected tissue samples were taken and processed for morphologic electron microscopy. The samples were fixed for 6 h in 2% glutaraldehyde in 0.1 mol/L cacodylate buffer, pH 7.2, supplemented with 0.1 mol/L sucrose. They then were fixed in 1% osmium tetroxide in the same buffer, dehydrated in a graded series of ethanol, immersed in propylene oxide, and infiltrated with epoxy resin (Agar 100; Agar Aids Scientific, Stansted, UK). Polymerization at 60°C followed. Ultrathin sections (60–80 nm) were placed on gilded grids coated with Formvar (Monsanto, St. Louis, MO) and contrasted for 30 min with 4% uranyl acetate and for 3 min with the lead citrate of Reynolds (16). Some grids were left for morphologic examination, and the rest were used for autoradiographic examination. L4 nuclear research emulsion (Ilford Anitec, Gothenburg, Sweden) for autoradiography was used after 1:5 dilution in distilled water. The emulsion gel was melted and diluted at 43°C . Grids were coated with film using the wire loop technique (16). After drying for 4 h, the grids were placed in a light-tight box containing silica gel and placed at 4°C . The exposure times were 2, 3, 4, and 7 d. The grids were developed for 3 min in D19 developer (Kodak AB, Järfälla, Sweden) and fixated for 6 min in Unifix (Kodak AB). As a negative control, a normal nonradioactive mouse pituitary specimen was included and handled in parallel with the tumor specimen.

RESULTS

Gross Tumor Radioactivity

The radioactivity of the tumor specimens was analyzed in a well counter, and the tissue-to-blood ratios were calculated. The tumor-to-blood ratios varied between 12 and 464 for the primary tumor and between 12 and 380 for the metastases.

Somatostatin Receptor Scintigraphy

In all patients, the carcinoid tumor could be visualized through preoperative somatostatin receptor scintigraphy. In 6 patients, metastatic lesions could also be seen (Fig. 1).

Morphologic Electron Microscopy

Morphologic examination with electron microscopy showed the carcinoid cells to grow in isletlike nests. The outermost peripheral parts of the tumor nests revealed cells with numerous heteromorphous hormone granules gathered in their basal parts (Fig. 2A). In these cells, a high endocytotic activity was evident by the presence of numerous clathrin-coated vesicles, uncoated vesicles, tubular systems, and endosomes (Fig. 2B). Active endocrine cells constituted a 2- to 6-cell border in the tumor nests. Cells in the more central part of the tumor nests contained comparably fewer granules (Fig. 2A), and plasma membranes facing the lumens were equipped with microvilli. Many tumor cells were in different stages of necrosis with condensed nuclear chromatin, swollen organelles, and large vacuoles (Fig. 2A). These affected cells either were scattered among nonnecrotic cells or composed pronounced parts of the cell mass in

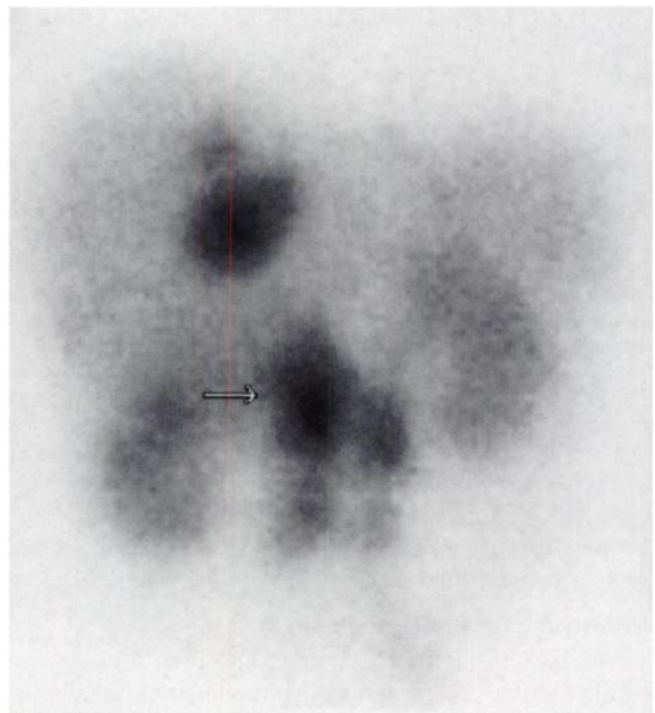


FIGURE 1. Reconstructed SPECT coronal view over abdomen of patient with midgut carcinoid tumor metastasized to liver. Primary tumor is indicated by arrow. Tumors were verified by surgery.

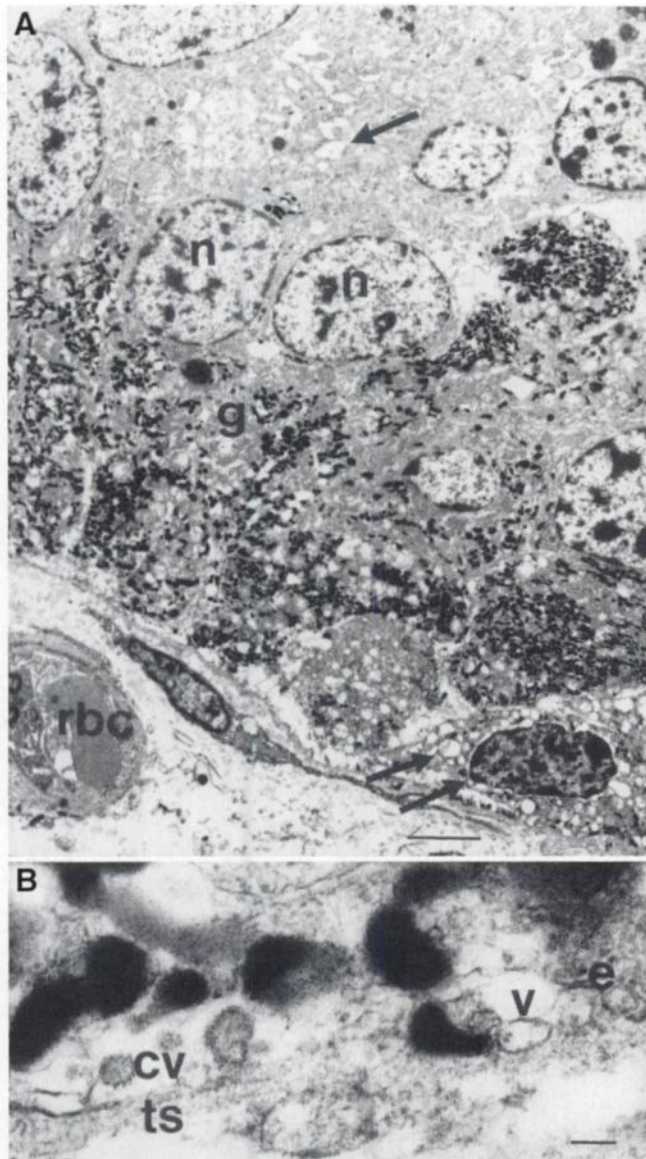


FIGURE 2. Morphologic electron microscopy survey. (A) Neuroendocrine tumor cells are seen growing in typical isletlike pattern. Tumor cells have round, moderately sized nuclei (n) with spotty pattern of chromatin. Heteromorphous secretory granules (g) are gathered in basal part of cells. Many cells show dilated vacuolar structures and nuclei with condensed chromatin (arrows). Blood capillary with red blood cell (rbc) is seen in bottom right corner. $\times 9000$; bar = 1000 nm. (B) Area within plasma membrane is rich in clathrin-coated vesicles (cv) and uncoated vesicles (v), tubular structures (ts), endosomes (e), and secretory granules. $\times 54,000$; bar = 100 nm.

central parts in the isletlike nests. Debris from dead cells was seen in the interstitial tissue.

Ultrastructural Autoradiography

The cells in the primary tumor and metastases showed similar activity in uptake and intracellular processing of ^{111}In -octreotide. The morphology of the autoradiographic sections was inferior in comparison with pure morphologic sections, but still, ultrastructural details were detectable. All endocrine tumor cells were convincingly labeled with the

^{111}In -octreotide silver grain reaction product (Fig. 3). Tumor cells bordering the stroma and blood vessels revealed higher uptake of ^{111}In -octreotide than did cells in the center of the isletlike formations. Silver grains showing the presence of internalized ^{111}In -octreotide were located on the plasma membrane and throughout the cytoplasm as well as in the perinuclear area (Figs. 4A–C). Most tumor cell nuclei showed nuclear localization of ^{111}In (Figs. 3 and 4D). The number of grains increased slightly with exposure duration.

After 2, 3, and 4 d of exposure, almost no silver grains were seen in other tissue or in cells other than the carcinoid cells. No grains were seen in the plastic. After 7 d of exposure, a few unspecific grains were seen. Control sections from the adjacent normal intestine and normal non-radioactive pituitary specimen were covered with film, exposed, and developed together with the ^{111}In -octreotide-labeled carcinoid sections and showed no silver grains.

DISCUSSION

Treatment with tumor-targeting radioactive agents is an interesting addition to the therapeutic arsenal for malignant

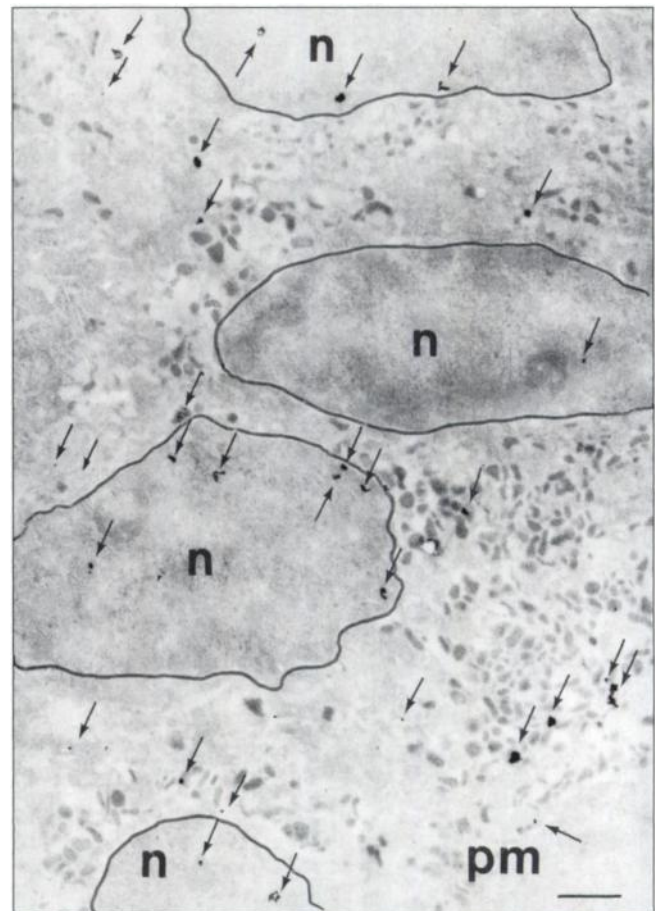


FIGURE 3. Low-magnification photomicrograph shows autoradiographic results in parts of 4 different cells in tumor cell cluster. Plasma membrane binding, receptor–ligand internalization, and further translocation are shown by several silver grains (arrows) on plasma membrane (pm), throughout cytoplasm and in nuclei (n). Membranes of 4 nuclei are outlined. Exposure was 7 d. $\times 8400$; bar = 1000 nm.

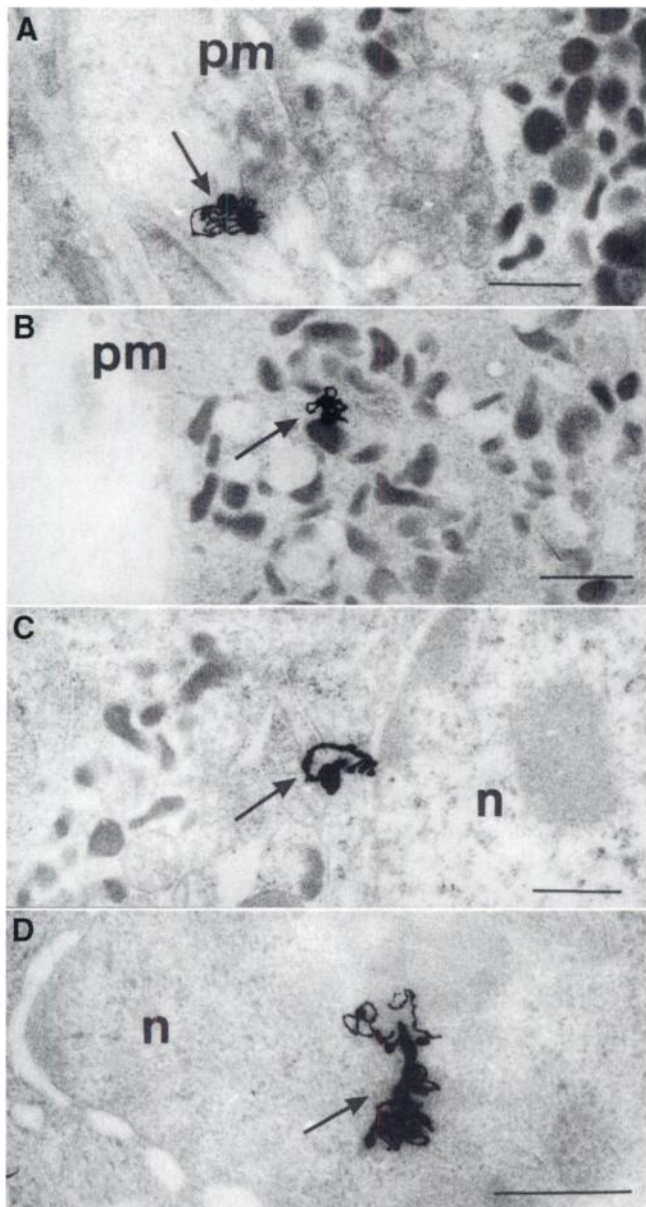


FIGURE 4. High-magnification photomicrograph reveals ^{111}In -octreotide (arrows) binding to somatostatin receptor on plasma membrane (A) and internalization in cell into, or in close vicinity of, vacuoles, which are mingled among secretory granules (B). Silver grains are also seen translocated to perinuclear area (C) and nucleus (D). Exposure was 4 or 7 d. $\times 24,000$ (A–C) and $\times 36,000$ (D); bars = 500 nm; n = nuclei; pm = plasma membrane.

tumors. Radiolabeled monoclonal antibodies have been tried for colonic cancer (17), and radioactively labeled metaiodobenzylguanidine (MIBG) has been tried for neuroblastomas (18). Somatostatin receptors as targets for radioactive therapy of neuroendocrine tumors have drawn much attention. However, the initial favorable clinical results have been difficult to explain because the γ -rays emitted by ^{111}In from a radiobiologic point of view are insufficient to account for an antitumoral effect. Interest has been directed toward the Auger electrons emitted by the isotope (13). The range for

these particles is much less than a cell diameter, and the isotope therefore has to be internalized into the cell to damage DNA and kill cells.

In vitro data support internalization of the somatostatin receptor–ligand complex (19–22). However, this study focuses on the more complex processes of in vivo surface binding and internalization of tracer amounts of ^{111}In -octreotide in carcinoid tumor cells after intravenous injection of the substance to patients with neuroendocrine tumors.

We report on an in vivo method for investigation of cellular uptake and intracellular distribution of a radioactive compound. We found the gross radioactivity uptake in the tumor—as compared with normal tissue and peripheral blood measured in a γ well counter—to be within the expected range for midgut carcinoid tumors (9,14). Because of the inferior resolution of the morphology, and because each silver grain emanates from a single ^{111}In -radionuclide reflecting an energy area with an unknown diameter, the exact intracellular location of the ^{111}In -octreotide molecule is difficult to decide. Grains were located in the vicinity of the plasma membrane area where morphologic examination revealed many endocytotic vesicles. These grains probably reflect octreotide cell surface binding to somatostatin receptors and further internalization to the endosomal compartments where the ligand is uncoupled and the receptor is recycled to the plasma membrane. Many silver grains were also located in the perinuclear area and within the nucleus, where they may reflect the final intracellular action of the radiolabeled octreotide molecule. Nuclear localization of the silver precipitations shows that the ^{111}In can actually reach the DNA molecule and thus provides evidence of the possible antitumor mechanism of ^{111}In -octreotide.

Our results agree with previous in vitro ultrastructural studies of octreotide uptake (19,22). However, the earlier reports declare a noticeably lower rate of binding and internalization than was found in our in vivo study. This difference may reflect a true discrepancy between in vivo and in vitro octreotide binding and uptake or may be caused by differences in techniques. Our in vivo findings on intracellular distribution of the isotope support the hypothesis of receptor–ligand internalization and the radiobiologic effect of Auger electrons in patients treated with high activities of ^{111}In -octreotide. Future studies need to address this question, and the presented method has the potential to increase our knowledge about this issue.

CONCLUSION

Together with [^{110}In -DTPA-D-Phe 1]-octreotide PET, the presented method may be used to solve questions about dose distribution and the heterogeneity of radioactivity distribution in tumors. The method may also contribute to future dose-planning studies for patients scheduled for ^{111}In -octreotide treatment. Today, the dose of radioactive compound injected for treatment is decided using data obtained by gamma camera scintigraphy and blood, urine, and feces

samples. With the method we describe, biopsies from metastases that accumulate tracer can be investigated and the amount of bound and internalized analog can be measured and used for microdosimetry. This ability can contribute to individual dose planning and help optimize radioactive treatment.

ACKNOWLEDGMENTS

This study was supported by the Swedish Society of Medicine, the Swedish Medical Research Council, the Lions Foundation for Cancer Research at the University Hospital in Uppsala, and the Swedish Cancer Foundation.

REFERENCES

1. Yamada Y, Post SR, Wang K, Tager HS, Bell GI, Seino S. Cloning and functional characterization of a family of human and mouse somatostatin receptors expressed in brain, gastrointestinal tract, and kidney. *Proc Natl Acad Sci USA*. 1992;89:251-255.
2. Yamada Y, Reisine T, Law SF, et al. Somatostatin receptors, an expanding gene family: cloning and functional characterization of human SSSTR3, a protein coupled to adenylyl cyclase. *Mol Endocrinol*. 1992;6:2136-2142.
3. Yamada Y, Kagimoto S, Kubota A, et al. Cloning, functional expression and pharmacological characterization of a fourth (hSSSTR4) and a fifth (hSSSTR5) human somatostatin receptor subtype. *Biochem Biophys Res Commun*. 1993;195:844-852.
4. Schaer JC, Waser B, Mengod G, Reubi JC. Somatostatin receptor subtypes sst1, sst2, sst3 and sst5 expression in human pituitary, gastroentero-pancreatic and mammary tumors: comparison of mRNA analysis with receptor autoradiography. *Int J Cancer*. 1997;70:530-537.
5. Reubi JC, Kvols LK, Waser B, et al. Detection of somatostatin receptors in surgical and percutaneous needle biopsy samples of carcinoids and islet cell carcinomas. *Cancer Res*. 1990;50:5969-5977.
6. Lamberts SWJ, van der Lely A-J, de Herder WW, Hofland LJ. Octreotide. *N Engl J Med*. 1996;334:246-254.
7. Krenning EP, Bakker WH, Kooij PPM, et al. Somatostatin receptor scintigraphy with indium-111-DTPA-D-Phe-1-octreotide in man: metabolism, dosimetry and comparison with iodine-123-Tyr-3-octreotide. *J Nucl Med*. 1992;33:652-658.
8. Janson ET, Westlin JE, Eriksson B, Ahlström H, Nilsson S, Öberg K. [¹¹¹In-DTPA-D-Phe¹]octreotide scintigraphy in patients with carcinoid tumors: the predictive value for somatostatin analogue treatment. *Eur J Endocrinol*. 1994;131:577-581.
9. Öhrvall U, Westlin JE, Nilsson S, et al. Human biodistribution of [¹¹¹In]diethylene-triaminepentaacetic acid (DTPA)-D-[Phe¹]octreotide and preoperative detection of endocrine tumors. *Cancer Res*. 1995;55:5794s-5800s.
10. Krenning EP, Kooij PP, Pauwels S, et al. Somatostatin receptor: scintigraphy and radionuclide therapy. *Digestion*. 1996;57(suppl 1):57-61.
11. McCarthy KE, Woltering EA, Espenan GD, Cronin M, Maloney TJ, Anthony LB. In situ radiotherapy with ¹¹¹In-pentetreotide: initial observations and future directions. *Cancer J Sci Am*. 1998;4:94-102.
12. Janson ET, Eriksson B, Öberg K, et al. Treatment with high dose Octreoscan in patients with neuroendocrine tumors: evaluation of therapeutic and toxic effects. *Acta Oncol*. 1999;38:373-377.
13. McLean JR, Blakey DH, Douglas GR, Bayley J. The Auger electron dosimetry of indium-111 in mammalian cells in vitro. *Radiat Res*. 1989;119:205-218.
14. Lukinius A, Öhrvall U, Westlin JE, Öberg K, Janson ET. In vivo cellular distribution and endocytosis of the somatostatin receptor-ligand complex. *Acta Oncol*. 1999;38:383-387.
15. Westlin JE, Janson ET, Ahlström H, Nilsson S, Öhrvall U, Öberg K. Scintigraphy using 111-indium labelled somatostatin analogue for localization of neuroendocrine tumors. *Antibiot Immunoconjug Radiopharm*. 1992;5:367-384.
16. Reynolds ES. The use of lead citrate at high pH as an electron opaque stain in electron microscopy. *J Cell Biol*. 1963;17:208-212.
17. Welt S, Divgi CR, Kemeny N, et al. Phase I/II study of iodine 131-labeled monoclonal antibody A33 in patients with advanced colon cancer. *J Clin Oncol*. 1994;12:1561-1571.
18. Hoefnagel CA. Radionuclide therapy revisited. *Eur J Nucl Med*. 1991;18:408-431.
19. Krisch B, Feindt J, Mentlein R. Immunoelectronmicroscopic analysis of the ligand-induced internalization of the somatostatin receptor subtype 2 in cultured human glioma cells. *J Histochem Cytochem*. 1998;46:1233-1242.
20. Koenig JA, Edwardson JM, Humphrey PPA. Somatostatin receptors in neuro2A neuroblastoma cells: ligand internalization. *Br J Pharm*. 1997;120:52-59.
21. Hofland LJ, Breeman WAP, Krenning EP, et al. Internalization of [DOTA⁰,¹²⁵I-Tyr¹]octreotide by somatostatin receptor positive cells in vitro and in vivo: implications for somatostatin receptor-targeted radioguided surgery. *Proc Assoc Am Physicians*. 1999;111:63-69.
22. Andersson P, Forsell-Aronsson E, Johansson V, et al. Internalization of indium-111 into human neuroendocrine tumor cells after incubation with indium-111-DTPA-D-Phe¹-octreotide. *J Nucl Med*. 1996;37:2002-2006.